Basic Principles of RF Superconductivity and Superconducting Cavities [1]

Peter Schmüser
Institut für Experimentalphysik
Universität Hamburg

Abstract

The basics of superconductivity are outlined with special emphasis on the features which are relevant for the application of superconductors in radio frequency cavities for particle acceleration. For a cylindrical resonator ("pill box cavity") the electromagnetic field in the cavity and important parameters such as resonance frequency, quality factor and shunt impedance are calculated analytically. The design and performance of practical cavities is shortly addressed.

1 Introduction

1.1 Advantages and limitations of superconductor technology in accelerators

The vanishing electrical resistance of superconducting coils as well as their ability to provide magnetic fields far beyond those of saturated iron is the main motivation for using superconducting (sc) magnets in all new large proton, antiproton and heavy ion accelerators[2]. Superconductivity does not only open the way to much higher particle energies but at the same time leads to a substantial reduction of operating costs. In the normal-conducting Super Proton Synchrotron SPS at CERN a power of 52 MW is needed to operate the machine at an energy of 315 GeV while at HERA a cryogenic plant with 6 MW electrical power consumption is sufficient to provide the cooling of the superconducting magnets with a stored proton beam of 920 GeV. Hadron energies in the TeV regime are practically inaccessible with standard magnet technology. Another important application of superconducting materials is in the large experiments at hadron or lepton colliders where superconducting detector magnets are far superior to normal magnets.

In the case of accelerating cavities the advantage of superconductors is not at all that obvious. In fact, three of the proposed linear electron positron colliders are based on copper acceleration structures: the 'Next Linear Collider' NLC [3] at Stanford, the 'Japanese Linear Collider' JLC [4] at Tsukuba, and the 'Compact Linear Collider' CLIC [5] at CERN, while only the international TESLA project [6, 7] uses sc niobium cavities. The traditional arguments against superconductor technology in linear colliders have been the low accelerating fields achieved in sc cavities and the high cost of cryogenic equipment. Superconducting cavities face a strong physical limitation: the microwave magnetic field must stay below the critical field of the superconductor. For the best superconductor for cavities, niobium, this corresponds to a maximum accelerating field of about 45 MV/m while normal-conducting cavities operating at high frequency (above 5 GHz) should in principle be able to reach 100 MV/m or more. In practice, however, sc cavities were often found to be limited at much lower fields of some 5 MV/m and hence were totally non-competitive for a linear collider. Great progress was achieved with the 340 five-cell cavities of the Continuous Electron Beam Accelerator Facility CEBAF [8] at Jefferson Laboratory in Virginia, USA. These 1.5 GHz niobium cavities were developed at Cornell University and produced by industry. They exceeded the design gradient of 5 MV/m and achieved 8.4 MV/m after installation in the accelerator (in several specially prepared cavities even 15-20 MV/m were reached). Building upon the CEBAF experience the intensive R&D of the TESLA collaboration has succeeded in raising the accelerating field in multicell cavities to more than 25 MV/m. There is a realistic chance to reach even 35 MV/m, and to reduce substantially the cost for the cryogenic installation.

While superconducting magnets operated with direct current are free of energy dissipation, this is not the case in microwave cavities. The non-superconducting electrons (see sect. 2) experience forced oscillations in the time-varying magnetic field and dissipate power in the material. Although the resulting heat deposition is many orders of magnitude smaller than in copper cavities it constitutes a significant heat load on the

[1] Adapted from a review article in Prog. Part. Nucl. Phys. [1].
[2] The parameters of high energy lepton and hadron colliders are summarized in [2].

refrigeration system. As a rule of thumb, 1 W of heat deposited at 2 K requires almost 1 kW of primary ac power in the refrigerator. Nevertheless, there is now a worldwide consensus that the overall efficiency for converting primary electric power into beam power is about a factor two higher for a superconducting than for a normal-conducting linear collider with optimized parameters in either case [9]. Another definite advantage of a superconducting collider is the low resonance frequency of the cavities that can be chosen (1.3 GHz in TESLA). The longitudinal (transverse) wake fields generated by the ultrashort electron bunches upon passing the cavities scale with the second (third) power of the frequency and are hence much smaller in TESLA than in NLC ($f = 11$ GHz). The wake fields may have a negative impact on the beam emittance (the area occupied in phase space) and on the luminosity of the collider.

1.2 Characteristic properties of superconducting cavities

The fundamental advantage of superconducting niobium cavities is the extremely low surface resistance of a few nano-ohms at 2 Kelvin as compared to several milli-ohms in copper cavities. The quality factor Q_0 (2π times the ratio of stored energy to energy loss per cycle) is inversely proportional to the surface resistance and may exceed 10^{10}. Only a tiny fraction of the incident radio frequency (rf) power is dissipated in the cavity walls, the lion's share is transferred to the beam. The physical limitation of a sc resonator is given by the requirement that the rf magnetic field at the inner surface has to stay below the critical field of the superconductor (about 190 mT for niobium), corresponding to an accelerating field of $E_{acc} = 45$ MV/m. In principle the quality factor should stay constant when approaching this fundamental superconductor limit but in practice the curve $Q_0 = Q_0(E_{acc})$ ends at considerably lower values, often accompanied with a strong decrease of Q_0 towards the highest gradient reached in the cavity. The main reasons for the performance degradation are excessive heating caused by impurities on the inner surface or by field emission of electrons. The cavity becomes partially normal-conducting, associated with strongly enhanced power dissipation. Because of the exponential increase of surface resistance with temperature this may result in a run-away effect and eventually a quench of the entire cavity.
Field emission of electrons from sharp tips is the most severe limitation in high-gradient superconducting cavities. Small particles on the cavity surface act as field emitters. By applying the clean room techniques developed in semiconductor industry it has been possible to raise the threshold for field emission in multicell cavities from about 10 MV/m to more than 20 MV/m in the past few years. The preparation of a smooth and almost mirror-like surface by electrolytic polishing is another important improvement.
A detailed description of sc cavities is found in [10].

2 Basics of Superconductivity

The unusual features of superconducting magnets and cavities are closely linked to the physical properties of the superconductor itself. For this reason a basic understanding of superconductivity is indispensable for the design, construction and operation of superconducting accelerator components. Only the traditional 'low-temperature' superconductors are treated since up to date the use of 'high-temperature' ceramic superconductors in these devices is rather limited [11, 12]. For more comprehensive presentations I refer to the excellent text books by W. Buckel [13] and by D.R. Tilley and J. Tilley [14].

2.1 Overview

Superconductivity - the infinitely high conductivity below a 'critical temperature' T_c - is observed in a large variety of materials but, remarkably, not in some of the best normal conductors like copper, silver and gold, except at very high pressures. This is illustrated in Fig. 1 where the resistivity of copper, tin and the 'high-temperature' superconductor $YBa_2Cu_3O_7$ is sketched as a function of temperature. Table 2.1 lists some important superconductors together with their critical temperatures at vanishing magnetic field.

There is an intimate relation between superconductivity and magnetic fields. W. Meissner and R. Ochsenfeld discovered in 1933 that a superconducting element like lead expels a weak magnetic field from

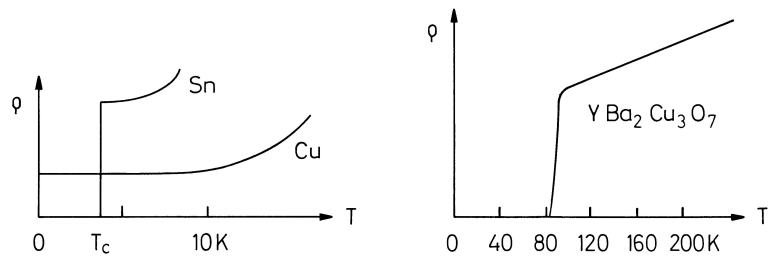

Figure 1: *The low-temperature resistivity of copper, tin and $YBa_2Cu_3O_7$.*

Al	Hg	Sn	Pb	Nb	Ti	NbTi	Nb_3Sn
1.14	4.15	3.72	7.9	9.2	0.4	9.4	18

Table 1: *Critical temperature T_c in K of selected superconducting materials for vanishing magnetic field.*

its interior when cooled below T_c, while in stronger fields superconductivity breaks down and the material goes to the normal state. The spontaneous exclusion of magnetic fields upon crossing T_c cannot be explained in terms of the Maxwell equations of classical electrodynamics and indeed turned out to be of quantum-theoretical origin. In 1935 H. and F. London proposed an equation which offered a phenomenological explanation of the field exclusion. The *London equation* relates the supercurrent density J_s to the magnetic field:

$$\vec{\nabla} \times \vec{J_s} = -\frac{n_s e^2}{m_e} \vec{B} \tag{1}$$

where n_s is the density of the super-electrons. In combination with the Maxwell equation $\vec{\nabla} \times \vec{B} = \mu_0 \vec{J_s}$ we get the following equation for the magnetic field in a superconductor

$$\nabla^2 \vec{B} - \frac{\mu_0 n_s e^2}{m_e} \vec{B} = 0 \, . \tag{2}$$

For a simple geometry, namely the boundary between a superconducting half space and vacuum, and with a magnetic field parallel to the surface, Eq. (2) reads

$$\frac{d^2 B_y}{dx^2} - \frac{1}{\lambda_L^2} B_y = 0 \quad \text{with} \quad \lambda_L = \sqrt{\frac{m_e}{\mu_0 n_s e^2}} \quad . \tag{3}$$

Here we have introduced a very important superconductor parameter, the *London penetration depth* λ_L. The solution of the differential equation is

$$B_y(x) = B_0 \exp(-x/\lambda_L) \, . \tag{4}$$

So the magnetic field does not abruptly drop to zero at the superconductor surface but penetrates into the material with exponential attenuation (Fig. 2). For typical material parameters the penetration depth is quite small, namely 20 – 50 nm. In the bulk of a thick superconductor the magnetic field vanishes which is just the Meissner-Ochsenfeld effect.

The justification of the London equation remained obscure until the advent of the microscopic theory of superconductivity by Bardeen, Cooper and Schrieffer in 1957. The BCS theory is based on the assumption that the supercurrent is not carried by single electrons but rather by pairs of electrons of opposite momenta and spins, the so-called *Cooper pairs*. The London penetration depth remains invariant under the replacements $n_s \to n_c = n_s/2$, $e \to 2e$ and $m_e \to m_c = 2m_e$. The BCS theory revolutionized our understanding of superconductivity. All Cooper pairs occupy a single quantum state, the BCS ground state, whose energy is

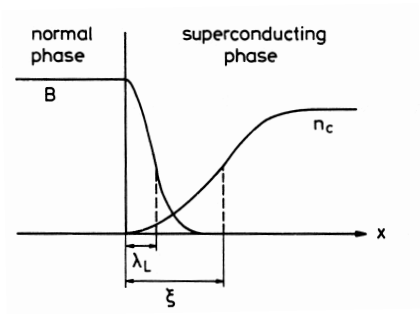

Figure 2: *The exponential drop of the magnetic field and the rise of the Cooper-pair density at a boundary between a normal and a superconductor.*

separated from the single-electron states by a temperature dependent energy gap $E_g = 2\,\Delta(T)$. The critical temperature is related to the energy gap at $T = 0$ by

$$1.76\,k_B T_c = \Delta(0)\ . \tag{5}$$

Here $k_B = 1.38 \cdot 10^{-23}$ J/K is the Boltzmann constant. The magnetic flux through a superconducting ring is found to be quantized, the smallest unit being the elementary flux quantum

$$\Phi_0 = \frac{h}{2e} = 2.07 \cdot 10^{-15}\ \mathrm{Vs}\ . \tag{6}$$

These and many other predictions of the BCS theory, like the temperature dependence of the energy gap and the existence of quantum interference phenomena, have been confirmed by experiment and often found practical application.

A discovery of enormous practical consequences was the finding that there exist two types of superconductors with rather different response to magnetic fields. The elements lead, mercury, tin, aluminium and others are called 'type I' superconductors. They do not admit a magnetic field in the bulk material and are in the superconducting state provided the applied field stays below a *critical field* H_c ($B_c = \mu_0 H_c$ is usually less than 0.1 Tesla). All superconducting alloys like lead-indium, niobium-titanium, niobium-tin and also the element niobium belong to the large class of 'type II' superconductors. They are characterized by two critical fields, H_{c1} and H_{c2}. Below H_{c1} these substances are in the *Meissner phase* with complete field expulsion while in the range $H_{c1} < H < H_{c2}$ they enter the *mixed phase* in which the magnetic field pierces the bulk material in the form of flux tubes. Many of these materials remain superconductive up to much higher fields (10 Tesla or more).

2.2 Energy balance in a magnetic field

A material like lead makes a phase transition from the normal to the superconducting state when it is cooled below T_c and when the magnetic field is less than $H_c(T)$. This is a phase transition comparable to the transition from water to ice below 0°C. Phase transitions take place when the new state is energetically favoured. The relevant thermodynamic energy is here the so-called Gibbs free energy G. Free energies have been measured for a variety of materials. For temperatures $T < T_c$ they are found to be lower in the superconducting than in the normal state while G_{sup} approaches G_{norm} in the limit $T \to T_c$, see Fig. 3a. What is now the impact of a magnetic field on the energy balance? A magnetic field has an energy density $\mu_0/2 \cdot H^2$, and according to the Meissner-Ochsenfeld effect the magnetic energy must be pushed out of the material when it enters the superconducting state. Hence the free energy per unit volume in the superconducting state increases quadratically with the applied field:

$$G_{sup}(H) = G_{sup}(0) + \frac{\mu_0}{2}\,H^2\ . \tag{7}$$

The normal-state energy remains unaffected. The material stays superconductive as long as $G_{sup}(H) < G_{norm}$. Equation (7) implies the existence of a maximum tolerable field, the 'critical field', above which superconductivity breaks down. It is defined by the condition that the free energies in the superconducting and in the normal state be equal

$$G_{sup}(H_c) = G_{norm} \;\Rightarrow\; \frac{\mu_0}{2} H_c^2 = G_{norm} - G_{sup}(0)\ . \tag{8}$$

Figure 3b illustrates what we have said. For $H > H_c$ the normal phase has a lower energy, so the material goes to the normal state. Equation (8) is also meaningful for type II superconductors and defines in this case the *thermodynamic critical field* which lies between H_{c1} and H_{c2}. The quantity $\mu_0/2 \cdot H_c^2 = G_{norm} - G_{sup}(0)$

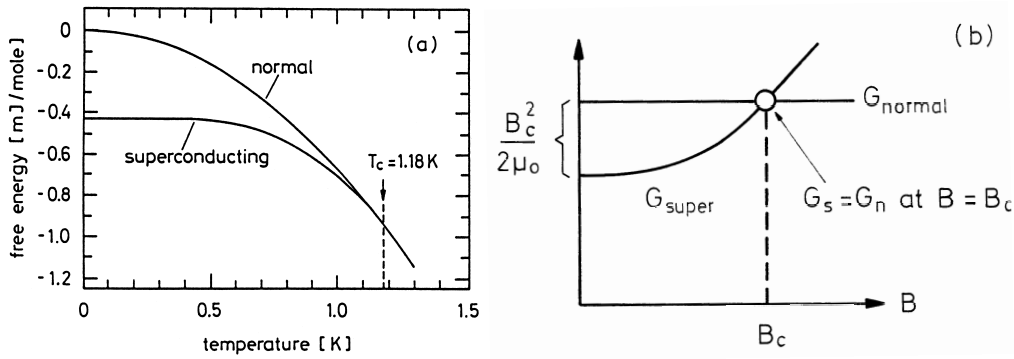

Figure 3: *(a) Free energy of aluminium in the normal and superconducting state as a function of T (after N.E. Phillips). The normal state is achieved by applying a magnetic field larger than B_c. (b) Schematic sketch of the free energies G_{norm} and G_{sup} as a function of the applied magnetic field $B = \mu_0 H$.*

can be interpreted as the Cooper-pair condensation energy per unit volume.

2.3 Coherence length and distinction between type I and type II superconductors

In very thin sheets of superconductor (thickness $< \lambda_L$) the magnetic field does not drop to zero at the centre. Consequently less magnetic energy needs to be expelled which implies that the critical field of a thin sheet may be much larger than the H_c of a thick slab. From this point of view it might appear energetically favourable for a thick slab to subdivide itself into an alternating sequence of thin normal and superconducting slices. The magnetic energy is indeed lowered that way but there is another energy to be taken into consideration, namely the energy required to create the normal-superconductor interfaces. At the boundary between the normal and the superconducting phase the density n_c of the super-current carriers (the Cooper pairs) does not jump abruptly from zero to its value in the bulk but rises smoothly over a finite length ξ, called *coherence length*, see Fig. 2.

The relative size of the London penetration depth λ_L and the coherence length ξ decides whether a material is a type I or a type II superconductor. Creation of a boundary means a loss of Cooper-pair condensation energy in a thickness ξ but a gain of magnetic energy in a thickness λ_L. There is a net energy gain if $\lambda_L > \xi$. So a subdivision of the superconductor into an alternating sequence of thin normal and superconducting slices is energetically favourable if the London penetration depth exceeds the coherence length.

A more refined treatment is provided by the Ginzburg-Landau theory (see e.g. [14]). Here one introduces the *Ginzburg-Landau parameter*

$$\kappa = \lambda_L/\xi\ . \tag{9}$$

The criterion for type I or II superconductivity is found to be

$$\begin{aligned} \text{type I:} \quad & \kappa < 1/\sqrt{2} \\ \text{type II:} \quad & \kappa > 1/\sqrt{2}. \end{aligned}$$

The following table lists the penetration depths and coherence lengths of some important superconducting elements. Niobium is a type II conductor but close to the border to type I, while indium, lead and tin are clearly in the type I class.

material	In	Pb	Sn	Nb
λ_L [nm]	24	32	≈ 30	32
ξ [nm]	360	510	≈ 170	39

The coherence length ξ is proportional to the mean free path of the conduction electrons in the metal. In alloys the mean free path is generally much shorter than in pure metals hence alloys are always type II conductors.

In reality a type II superconductor is not subdivided into thin slices but the field penetrates the sample in the form of flux tubes which arrange themselves in a triangular pattern which can be made visible by evaporating iron atoms onto a superconductor surface sticking out of the liquid helium. The fluxoid pattern shown in Fig. 4a proves beyond any doubt that niobium is indeed a type II superconductor. Each flux tube or *fluxoid* contains one elementary flux quantum Φ_0 which is surrounded by a Cooper-pair vortex current. The centre of a fluxoid is normal-conducting and covers an area of roughly $\pi\xi^2$. When we apply an external field H, fluxoids keep moving into the specimen until their average magnetic flux density is identical to $B = \mu_0 H$. The fluxoid spacing in the triangular lattice $d = \sqrt{2\Phi_0/(\sqrt{3}B)}$ amounts to 20 nm at 6 Tesla. The upper critical field is reached when the current vortices of the fluxoids start touching each other at which point superconductivity breaks down. In the Ginzburg-Landau theory the upper critical field is given by

$$B_{c2} = \sqrt{2}\,\kappa\,B_c = \frac{\Phi_0}{2\pi\xi^2}\,. \tag{10}$$

For niobium-titanium with an upper critical field $B_{c2} = 14$ T this formula yields $\xi = 5\,\mathrm{nm}$. The coherence length is larger than the typical width of a grain boundary in NbTi which means that the supercurrent can freely move from grain to grain. In high-T_c superconductors the coherence length is often shorter than the grain boundary width, and then current flow from one grain to the next is strongly impeded.

2.4 Flux flow resistance and flux pinning

For application in accelerator magnets a superconducting wire must be able to carry a large current in the presence of a field of 5 – 10 Tesla. Type I superconductors are definitely ruled out because their critical field is far too low (below 0.1 Tesla). Type II conductors appear promising at first sight: they feature large upper critical fields, and high currents are permitted to flow in the bulk material. However there is the problem of *flux flow resistance*. A current flowing through an ideal type II superconductor, which is exposed to a magnetic field, exerts a Lorentz force on the flux lines and causes them to move through the specimen, see Fig. 4b. This is a viscous motion and leads to heat generation. So although the current itself flows without dissipation the sample acts as if it had an Ohmic resistance. The statement is even formally correct. The moving fluxoids represent a moving magnetic field which, according to theory of special relativity, is equivalent to an electric field $\vec{E}_{equiv} = \vec{B} \times \vec{v}/c^2$. It is easy to see that $\vec{E}_{equiv}$ and $\vec{J}$ point in the same direction just like in a normal resistor. To obtain useful wires for magnet coils flux flow has to be prevented by capturing the fluxoids at *pinning centres*. These are defects or impurities in the regular crystal lattice. The most important pinning centres in niobium-titanium are normal-conducting titanium precipitates in the so-called α phase whose size is in the range of the fluxoid spacing ($\approx$ 10 nm at 6 Tesla). Figure 5 shows a microscopic picture of a conductor with very high current density (3700 A/mm^2 at 5 T and 4.2 K).

A type II superconductor with strong pinning is called a *hard superconductor*. Hard superconductors are very well suited for high-field magnets, they permit dissipationless current flow in high magnetic fields. There is a penalty, however: these conductors exhibit a strong magnetic hysteresis which is the origin of the very annoying 'persistent-current' multipoles in superconducting accelerator magnets.

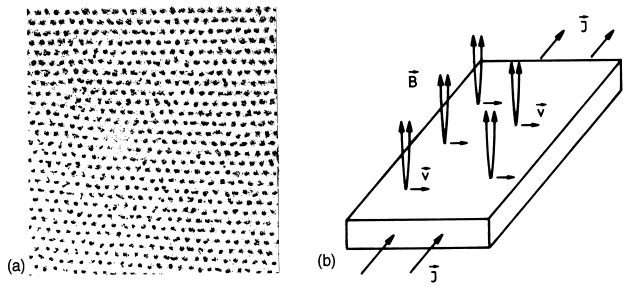

Figure 4: *(a) Fluxoid pattern in niobium (courtesy U. Essmann). The distance between adjacent flux tubes is 0.2 μm. (b) Fluxoid motion in a current-carrying type II superconductor.*

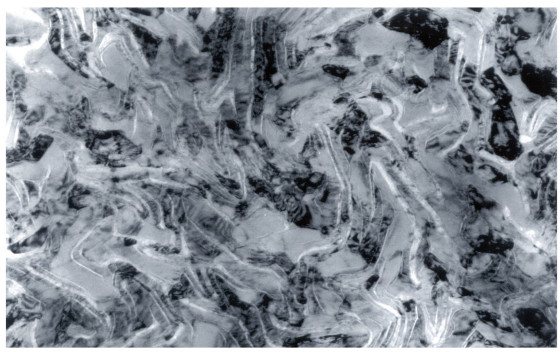

Figure 5: *Micrograph of NbTi. The α-titanium precipitates appear as lighter strips. The area covered is 840 nm wide and 525 nm high. Courtesy P.J. Lee and D.C. Larbalestier.*

2.5 Magnetization of a hard superconductor

A type I superconductor shows a reversible response[3] to a varying external magnetic field H. The magnetization is given by the straight line $M(H) = -H$ for $0 < H < H_c$ and then drops to zero. An ideal type II conductor without any flux pinning should also react reversibly. A hard superconductor, on the other hand, is only reversible in the Meissner phase because then no magnetic field enters the bulk, so no flux pinning can happen. If the field is raised beyond H_{c1} magnetic flux enters the sample and is captured at pinning centres. When the field is reduced again these flux lines remain bound and the specimen keeps a frozen-in magnetization even for vanishing external field. One has to invert the field polarity to achieve $M = 0$ but the initial state ($H = 0$ and no captured flux in the bulk material) can only be recovered by warming up the specimen to destroy superconductivity and release all pinned flux quanta, and by cooling down again.

A typical hysteresis curve is shown in Fig. 6. There is a close resemblence with the hysteresis in iron except for the sign: the magnetization in a superconductor is opposed to the magnetizing field because the physical mechanism is diamagnetism. The magnetic hysteresis is associated with energy dissipation. When a hard superconductor is exposed to a time-varying field and undergoes a cycle like the loop in Fig. 6, the energy loss is given by the integral

$$Q_{hyst} = \oint \mu_0 M(H) dH \ . \tag{11}$$

It is equal to the area enclosed by the loop. This energy must be provided by the power supply of the field-generating magnet and is transformed into heat in the superconductor when magnetic flux quanta are moved in and out of the specimen.

[3]This statement applies only for long cylindral or elliptical samples oriented parallel to the field.

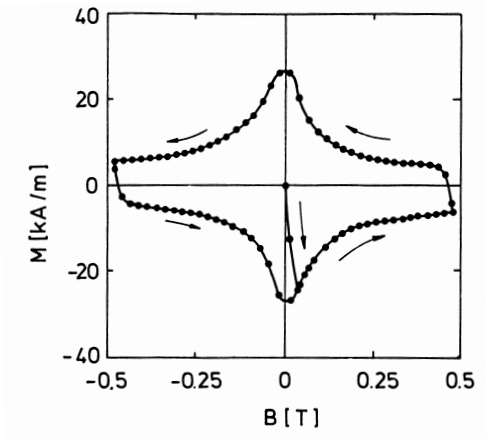

Figure 6: *Measured magnetization M of a multifilamentary niobium-titanium conductor [15]. Shown is the initial excitation, starting at $B = \mu_0 H = 0$ and $M = 0$, and the magnetic hysteresis for an external field B varying between +0.5 T and -0.5 T. Note that the hysteresis curve is not exactly symmetric with respect to the horizontal axis. The slight asymmetry is due to surface currents (Meissner-Ochsenfeld effect) whose magnetic moment is always opposed to the applied field.*

2.6 Critical current density

For a hard superconductor, not only temperature T and magnetic field H have to be specified but also current density J. The material can be conveniently characterized by its *critical surface* in a (T, H, J) coordinate system. For the most important conductor used in magnets, niobium-titanium, this surface is depicted in Fig. 7. Superconductivity prevails everywhere below the surface and normal conductivity above it. A hard superconductor is not exactly free of any resistance. The critical current density (at a given temperature and field) is usually defined by the criterion that the resistivity be $\rho = \rho_c = 10^{-14}\,\Omega$m. In the vicinity of this point the resistivity is a very steep function of current density. It can be parametrised with a power law

$$\rho(J) = \rho_c \left(\frac{J}{J_c}\right)^n \quad . \tag{12}$$

The exponent n is a quality index which may be as large as 50 for a good multifilamentary NbTi conductor.

2.7 Superconductors in microwave fields

Superconductivity in microwave fields is not treated adequately in standard text books. For this reason I present in this section a simplified explanation of the important concepts. A similar treatment can be found in [10]. Superconductors are free from energy dissipation in direct-current (dc) applications, but this is no longer true for alternating currents (ac) and particularly not in microwave fields. The reason is that the high-frequency magnetic field penetrates a thin surface layer and induces oscillations of the electrons which are not bound in Cooper pairs. The power dissipation caused by the motion of the unpaired electrons can be characterized by a surface resistance. In copper cavities the surface resistance is given by (see sect. 3.2.3)

$$R_{surf} = \frac{1}{\delta\sigma} \tag{13}$$

where δ is the skin depth and σ the conductivity of the metal.

The response of a superconductor to an ac field can be understood in the framework of the *two-fluid model*[4]. An ac current in a superconductor is carried by Cooper pairs (the superfluid component) as well as

[4]A similar model is used to explain the peculiar properties of liquid helium below 2.17 K.

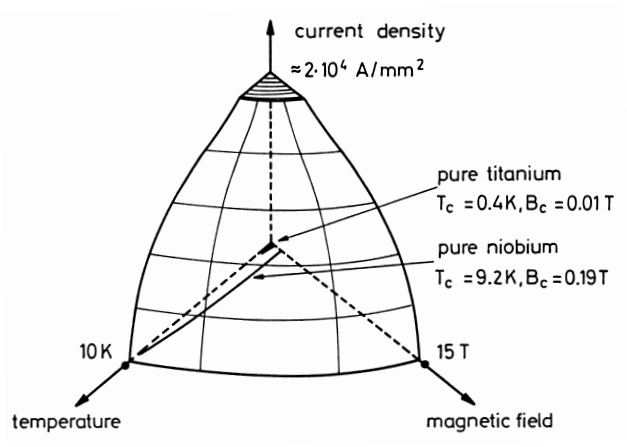

Figure 7: *Sketch of the critical surface of NbTi. Also indicated are the regions where pure niobium and pure titanium are superconducting. The critical surface has been truncated in the regime of very low temperatures and fields where only sparse data are available.*

by unpaired electrons (the normal component). Let us study the response to a periodic electric field. The normal current obeys Ohm's law

$$J_n = \sigma_n \, E_0 \, \exp(-i\omega t) \tag{14}$$

while the Cooper pairs receive an acceleration $m_c \, \dot{v}_c = -2e \, E_0 \, \exp(-i\omega t)$, so the supercurrent density becomes

$$J_s = i \, \frac{n_c \, 2 \, e^2}{m_e \omega} E_0 \, \exp(-i\omega t) \; . \tag{15}$$

If we write for the total current density

$$J = J_n + J_s = \sigma E_0 \exp(-i\omega t) \tag{16}$$

we get a complex conductivity:

$$\sigma = \sigma_n + i\sigma_s \quad \text{with} \quad \sigma_s = \frac{2 \, n_c e^2}{m_e \, \omega} = \frac{1}{\mu_0 \lambda_L^2 \, \omega} \; . \tag{17}$$

We know already that the rf magnetic field penetrates a superconductor much less than a normal conductor, namely only to a depth λ_L. The surface resistance is the real part of the complex surface impedance

$$R_{surf} = Re \left(\frac{1}{\lambda_L (\sigma_n + i\sigma_s)} \right) = \frac{1}{\lambda_L} \cdot \frac{\sigma_n}{\sigma_n^2 + \sigma_s^2} \; . \tag{18}$$

Since $\sigma_n^2 \ll \sigma_s^2$ at microwave frequencies one can disregard σ_n^2 in the denominator and obtains $R_{surf} \propto \sigma_n / (\lambda_L \sigma_s^2)$. So we arrive at the surprising result that the microwave surface *resistance* is proportional to the normal-state *conductivity*.
The conductivity of a normal metal is given by the classic Drude expression

$$\sigma_n = \frac{n_n e^2 \ell}{m_e v_F} \tag{19}$$

where n_n is the density of the unpaired electrons, ℓ their mean free path and v_F the Fermi velocity. The normal electrons are created by thermal breakup of Cooper pairs. There is an energy gap $E_g = 2\Delta(T)$

between the BCS ground state and the free electron states. By analogy with the conductivity of an intrinsic (undoped) semiconductor we get $n_n \propto \exp(-E_g/(2k_BT))$ and hence

$$\sigma_n \propto \ell \exp(-\Delta(T)/(k_BT)) . \tag{20}$$

Using $1/\sigma_s = \mu_0\lambda_L^2\omega$ and $\Delta(T) \approx \Delta(0) = 1.76k_BT_c$ we finally obtain for the BCS surface resistance

$$R_{BCS} \propto \lambda_L^3\,\omega^2\,\ell \exp(-1.76\,T_c/T) . \tag{21}$$

This formula displays two important aspects of microwave superconductivity: the surface resistance depends exponentially on temperature, and it is proportional to the square of the rf frequency.

3 Design Principles and Properties of Superconducting Cavities

3.1 Choice of superconductor

In principle the critical temperature of the superconductor should be as high as possible. However, copper cavities coated with a high-T_c superconductor layer have shown unsatisfactory performance [11], therefore the helium-cooled low-T_c superconductors are applied. In contrast to magnets were hard superconductors with large upper critical field (10–20 T) are needed, the superconductor in microwave applications is not limited by the upper critical field but rather by the thermodynamic critical field (or possibly the 'superheating field') which is well below 0.5 T for all known superconducting elements and alloys. Moreover, strong flux pinning appears undesirable as it is coupled with hysteretic losses. Hence a 'soft' superconductor must be used, and pure niobium is the best candidate although its critical temperature is only 9.2 K and the thermodynamic critical field about 190 mT. Niobium-tin (Nb_3Sn) may appear more favorable since it has a higher critical temperature of 18 K and a superheating field of 400 mT; however, the gradients achieved in Nb_3Sn coated copper cavities were below 15 MV/m, probably due to grain boundary effects in the Nb_3Sn layer [16]. For these reasons pure niobium has been chosen in all large scale installations of sc cavities. There remain two choices for the cavity layout: the cavity is made from copper and the inner surface is coated with a thin layer of Nb or, alternatively, the cavity is made from solid Nb. The former approach has been taken with great success with the 350 MHz cavities of the Large Electron Positron ring LEP at CERN. In the TESLA linear collider, however, gradients of more than 25 MV/m are needed, and these are presently only accessible with cavities made from solid niobium. A high thermal conductivity is needed to guide the heat generated at the inner cavity surface through the wall to the liquid helium coolant. For this reason, the material must be of extreme purity with contaminations in the ppm range.

The BCS surface resistance is given by eq. (21). The exponential temperature depence is experimentally verified, see Fig. 8. For niobium the surface resistance at 1.3 GHz amounts to about 800 nΩ at 4.2 K and drops to 15 nΩ at 2 K. Operation at 2 K is essential for achieving high accelerating gradients in combination with very high quality factors. Superfluid helium is an excellent coolant owing to its high heat conductivity. In addition to the BCS term there is a residual resistance caused by impurities, frozen-in magnetic flux or lattice distortions.

$$R_{surf} = R_{BCS} + R_{res} . \tag{22}$$

R_{res} is temperature independent and amounts to a few nΩ for a clean niobium surface but may readily increase if the surface is contaminated.

Formula (21) applies if the mean free path ℓ of the unpaired electrons is much larger than the coherence length ξ. In niobium this condition is usually not fulfilled and one has to replace λ_L in the above equation by [17]

$$\Lambda = \lambda_L\sqrt{1+\xi/\ell} . \tag{23}$$

Combining equations (21) and (23) we arrive at the surprising statement that the surface resistance does not assume its minimum value when the superconductor is of very high purity ($\ell \gg \xi$) but rather of moderate

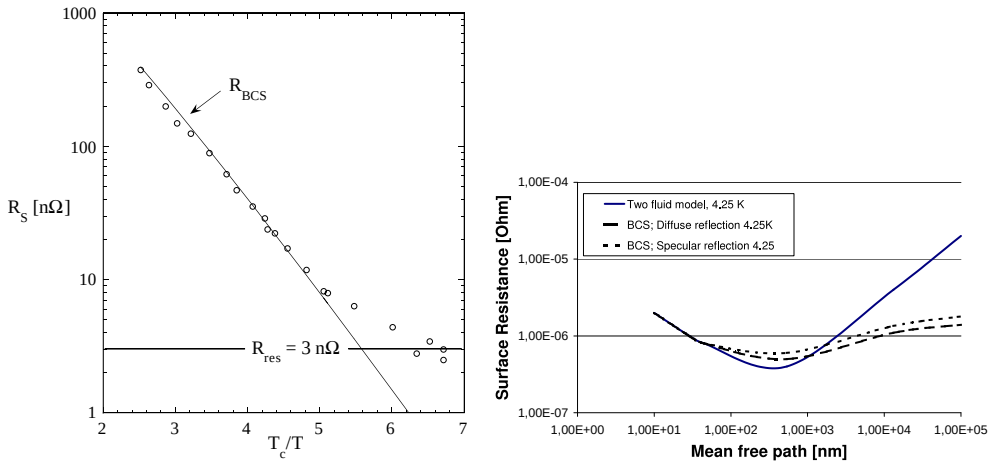

Figure 8: *Left: The surface resistance of a 9-cell TESLA cavity plotted as a function of T_c/T. The residual resistance of 3 nΩ corresponds to a quality factor $Q_0 = 10^{11}$. Right: The microwave surface resistance of niobium as a function of the mean free path ℓ of the unpaired electrons for a temperature of 4.25 K. Solid curve: two-fluid model; dashed curves: model calculations by Halbritter [18] based on the BCS theory.*

purity with a mean free path $\ell \approx \xi$, see Fig. 8. The measured BCS resistance in the sputter-coated LEP cavities is in fact a factor of two lower than in bulk niobium cavities [19]. The sputtered niobium layer has a low RRR (see sect. 3.6) and an electron mean free path $\ell \approx \xi$.

3.2 Pill box cavity

The simplest model of an accelerating cavity is a hollow cylinder which is often called pill box. When the beam pipes are neglected the field pattern inside the resonator and all relevant cavity parameters can be calculated analytically.

3.2.1 Field pattern

For particle acceleration we need a longitudinal electric field on the axis, hence we look for TM (transverse magnetic) eigenmodes of the cylindrical resonator. The field lines are sketched in Fig. 9. We use cylindrical

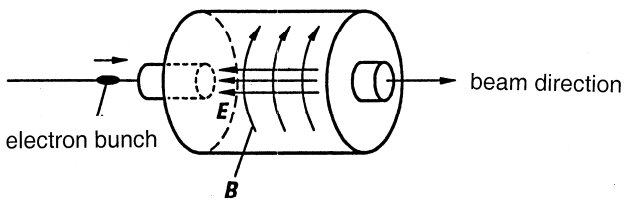

Figure 9: *Electric and magnetic field in a pillbox cavity for the accelerating mode TM_{010}.*

coordinates (r, θ, z) where z denotes the beam direction (cavity axis), $r = \sqrt{x^2 + y^2}$ the distance from the axis and θ the azimuthal angle. We search for an eigenmode with cylindrical symmetry (independence of θ) and with longitudinal electric and azimuthal magnetic field. The wave equation for the electric field reads

$$\frac{\partial^2 E_z}{\partial r^2} + \frac{1}{r}\frac{\partial E_z}{\partial r} = \frac{1}{c^2}\frac{\partial^2 E_z}{\partial t^2} \,. \tag{24}$$

For a harmonic time dependence $E_z(r)\cos(\omega t)$ and with the new variable $u = r\omega/c$ one obtains

$$\frac{\partial^2 E_z}{\partial u^2} + \frac{1}{u}\frac{\partial E_z}{\partial u} + E_z(u) = 0\,. \tag{25}$$

This is the Bessel equation of zero order with the solution $J_0(u)$. Hence the radial dependence of the electric field is

$$E_z(r) = E_0 J_0(\frac{\omega r}{c})\,. \tag{26}$$

For a perfectly conducting cylinder of radius R_c the longitudinal electric field must vanish at $r = R_c$, so $J_0(\omega R_c/c) = 0$. The first zero of $J_0(u)$ is at $u = 2.405$. This defines the frequency of the lowest eigenmode (we call it the fundamental mode in the following):

$$f_0 = \frac{2.405c}{2\pi R_c}\,, \quad \omega_0 = \frac{2.405c}{R_c}\ . \tag{27}$$

In a cylindrical cavity the frequency does not depend on the length L_c. The magnetic field can be computed from the equation

$$\frac{\partial E_z}{\partial r} = \mu_0 \frac{\partial H_\theta}{\partial t}\,. \tag{28}$$

Hence we obtain for the fundamental TM mode

$$\begin{aligned} E_z(r,t) &= E_0 J_0(\frac{\omega_0 r}{c})\cos(\omega_0 t)\,, \\ H_\theta(r,t) &= -\frac{E_0}{\mu_0 c} J_1(\frac{\omega_0 r}{c})\sin(\omega_0 t)\,. \end{aligned} \tag{29}$$

Electric and magnetic field are 90° out of phase. The azimuthal magnetic field vanishes on the axis and assumes its maximum close to the cavity wall.

3.2.2 Stored energy

The electromagnetic field energy is computed by integrating the energy density $(\varepsilon_0/2)E^2$ (at time $t = 0$) over the volume of the cavity. This yields

$$\begin{aligned} U &= \frac{\varepsilon_0}{2} 2\pi L_c E_0^2 \int_0^{R_c} J_0^2(\frac{\omega_0 r}{c}) r dr \\ &= \frac{\varepsilon_0}{2} 2\pi L_c E_0^2 \left(\frac{c}{\omega_0}\right)^2 \int_0^a J_0^2(u) u du \end{aligned} \tag{30}$$

where $a = 2.405$ is the first zero of J_0. Using the relation $\int_0^a J_0^2(u)udu = 0.5(aJ_1(a))^2$ we get for the energy stored in the cavity

$$U = \frac{\varepsilon_0}{2} E_0^2 (J_1(2.405))^2 \pi R_c^2 L_c\,. \tag{31}$$

3.2.3 Power dissipation in the cavity

We consider first a cavity made from copper. The rf electric field causes basically no losses since its tangential component vanishes at the cavity wall while the azimuthal magnetic field penetrates into the wall with exponential attenuation and induces currents within the skin depth[5]. These alternating currents give rise to Ohmic heat generation. The skin depth is given by

$$\delta = \sqrt{\frac{2}{\mu_0 \omega \sigma}} \tag{32}$$

[5]For a thorough discussion of the skin effect see J.D. Jackson, Classical Electrodynamics, chapt. 8.

where σ is the conductivity of the metal. For copper at room temperature and a frequency of 1 GHz the skin depth is $\delta = 2\mu$m. Consider now a small surface element. From Ampere's law $\oint \vec{H} \cdot \vec{ds} = I$ follows that the current density in the skin depth is related to the azimuthal magnetic field by $j = H_\theta/\delta$. Then the dissipated power per unit area is[6]

$$\frac{dP_{diss}}{dA} = \frac{1}{2\sigma\delta} H_\theta^2 = \frac{1}{2} R_{surf} H_\theta^2 \,. \tag{33}$$

Here we have introduced a very important quantity for rf cavities, the *surface resistance*:

$$R_{surf} = \frac{1}{\sigma\delta} \,. \tag{34}$$

In a superconducting cavity R_{surf} is given by equations (21) to (22). The power density has to be integrated over the whole inner surface of the cavity. This is straightforward for the cylindrical mantle where $H_\theta = \frac{E_0}{\mu_0 c} J_1(\omega_0 R/c)$ is constant. To compute the power dissipation in the circular end plates one has to evaluate the integral $\int_0^a (J_1(u))^2 u du = a^2 (J_1(a))^2/2$. Again $a = 2.405$ is the first zero of J_0. The total dissipated power in the cavity walls is then

$$P_{diss} = R_{surf} \cdot \frac{E_0^2}{2\,\mu_0^2\, c^2} (J_1(2.405))^2\, 2\pi R_c\, L_c\, (1 + R_c/L_c) \,. \tag{35}$$

3.2.4 Quality factor

The quality factor is an important parameter of a resonating cavity. It is defined as 2π times the number of cycles needed to dissipate the stored energy, or, alternatively, as the ratio of resonance frequency f_0 to the full width at half height Δf of the resonance curve

$$Q_0 = 2\pi \cdot \frac{U\, f_0}{P_{diss}} = \frac{f_0}{\Delta f} \,. \tag{36}$$

Using the formulas (31) and (35) we get the important equation

$$Q_0 = \frac{G}{R_{surf}} \quad \text{with} \quad G = \frac{2.405\,\mu_0\, c}{2(1 + R_c/L_c)} \tag{37}$$

which states that the quality factor of a cavity is obtained by dividing the so-called 'geometry constant' G by the surface resistance. G depends only on the shape of the cavity and not on the material. A typical value is 300 Ω. We want to point out that the quality factor Q_0 defined here is the intrinsic or 'unloaded' quality factor of a cavity. If the cavity is connected to an external load resistor by means of a coupler another quality factor (Q_{ext}) has to be introduced to account for the energy extraction through the coupler.

3.2.5 Accelerating field, peak electric and magnetic fields

A relativistic particle needs a time L_c/c to travel through the cavity. During this time the longitudinal electric field changes. The accelerating field is defined as the average field seen by the particle

$$E_{acc} = \frac{1}{L_c} \int_{-L_c/2}^{L_c/2} E_0 \cos(\omega_0 z/c) dz \,, \quad V_{acc} = E_{acc}\, L_c \,. \tag{38}$$

Choosing a cell length of one half the rf wavelength, $L_c = c/(2f_0)$, we get $E_{acc} = 0.64\, E_0$ for a pill box cavity.
The peak electric field at the cavity wall is E_0. The peak magnetic follows from eq. (29). We get

$$E_{peak}/E_{acc} = 1.57 \,, \; B_{peak}/E_{acc} = 2.7\,\mathrm{mT/(MV/m)} \,. \tag{39}$$

If one adds beam pipes to the cavity these number increase by 20 - 30%.

[6] In equation (33) the quantity H_θ denotes the amplitude of the magnetic field without the periodic time factor $\sin(\omega_0 t)$.

3.3 Shunt Impedance

To understand how the rf power coming from the klystron is transferred through the cavity to the particle beam it is convenient to represent the cavity by an equivalent parallel LCR circuit. The parallel Ohmic resistor is called the *shunt impedance* R_{shunt} although this quantity has only a real part. The relation between the peak voltage in the equivalent circuit and the accelerating field in the cavity is

$$V_0 = V_{acc} = E_{acc} L_c \; .$$

The power dissipated in the LCR circuit is

$$P_{diss} = \frac{V_0^2}{2R_{shunt}}$$

Identifying this with the dissipated power in the cavity, eq. (35), we get the following expression for the shunt impedance of a pillbox cavity[7]

$$R_{shunt} = \frac{2L_c^2 \mu_0^2 c^2}{\pi^3 (J_1(2.405))^2 R_c (R_c + L_c)} \cdot \frac{1}{R_{surf}} \; . \tag{40}$$

The surface resistance of a superconducting cavity is extremely small, about 15 nΩ at 2 K; consequently, the shunt impedance is extremely large, in the order of $5 \cdot 10^{12}$ Ω. Note that "on resonance" ($\omega = \omega_0 = 1/\sqrt{LC}$) the parallel LCR circuit behaves like a purely Ohmic resistor whose value is equal to the shunt impedance. The ratio of shunt impedance to quality factor is an important cavity parameter

$$(R/Q) \equiv \frac{R_{shunt}}{Q_0} = \frac{4L_c \mu_0 c}{\pi^3 (J_1(2.405))^2 2.405 R_c} \tag{41}$$

The (R/Q) parameter is independent of the material, it depends only on the shape of the cavity. A typical value for a 1-cell cavity is $(R/Q) = 100$ Ω.

3.4 Shape of practical cavities

The first sc cavities were built in the late 1960's with the conventional pill-box shape. They showed unexpected performance limitations: at field levels of a few MV/m a phenomen called multiple impacting (or *multipacting* for short) was observed. The effect is as follows: stray electrons which are released from the wall (for instance by cosmic rays) gain energy in one half-period of the electromagnetic field and return to their origin in the next half period were they impinge with a few 100 eV onto the wall and release secondary electrons which repeat the same procedure. This way an avalanche of electrons is created which absorbs energy from the rf field, heats the superconductor and eventually leads to a breakdown of superconductivity. It was found out many years later that this problem is avoided in cavities having the shape of a rotational ellipsoid. When electrons are emitted near the iris of an elliptical cavity and accelerated by the rf field, they return to a point away from their origin in the next half period, and the same applies for the possible next generations of electrons. Thereby the daughter electrons move more and more into the equator region where the rf electric field is small and the multiplication process dies out. For a thorough discussion I refer to [10].

In electron-positron storage rings quite often single-cell cavities are used. These are particularly well suited for the large beam currents of up to 1 A in the high luminosity 'B meson factories'. At larger energies like in LEP (104 GeV per beam) multicell cavities are more efficient to compensate for the huge synchrotron radiation losses (3 GeV per revolution in LEP). In a linear collider almost the full length of the machine must be filled with accelerating structures and then long multicell cavities are mandatory. There are, however, several effects which limit the number of cells N_c per resonator. With increasing N_c it becomes more and more difficult to tune the resonator for equal field amplitude in every cell. Secondly, in a very long multicell

[7] R_{shunt} is often defined by $P_{diss} = V_0^2/R_{shunt}$, then the (R/Q) parameter is a factor of 2 larger.

cavity 'trapped modes' may be excited by the short particle bunches. These are coupled oscillations at high frequency which are eam pipe sections that they cannot be gative influence on the following bunche ears a reasonable upper limit. The TE

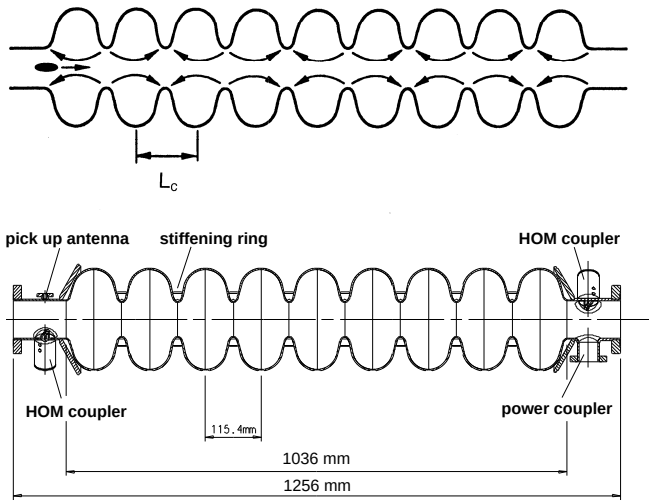

Figure 10: *Top: Schematic cross section of the 1 m long 9-cell TESLA cavity with electric field lines. The resonance frequency is 1.3 GHz and the cavity is operated in the π mode with 180° phase advance of the rf wave from cell to cell. The cell length equals 1/2 the rf wavelength so that relativistic electrons recieve the same energy gain in each cell. Bottom: Technical layout of the TESLA cavity with stiffening rings between neighbouring cells, two higher-order mode (HOM) couplers and flanges for mounting the rf power coupler and the pick-up antenna.*

Superconducting cavities are always operated in standing-wave mode[8]. The fundamental TM_{010} mode is chosen with a longitudinal electric field on the axis. In a cavity with N_c cells the fundamental mode splits into N_c coupled modes. The π mode with 180° phase difference between adjacent cells transfers the highest possible energy to the particles. The cell length L_c is determined by the condition that the electric field has to be inverted in the time a relativistic particle needs to travel from one cell to the next, so $L_c = c/(2f_0)$. For nonrelativistic protons or ions the cell length is $L_c = v/(2f_0)$. The iris radius influences the cell-to-cell coupling parameter k_{cell} which is in the order of 1 - 2 %. The frequencies of the coupled modes are given by the formula

$$f_m = \frac{f_0}{\sqrt{1 + 2\,k_{cell}\cos(m\pi/N_c)}}\,, \quad 1 \le m \le N_c\,. \tag{42}$$

3.5 Choice of frequency

The losses in a microwave cavity are proportional to the product of conductor area and surface resistance. For a given length of a multicell resonator, the area scales with $1/f$ while the surface resistance scales with f^2 for $R_{BCS} \gg R_{res}$ (see eq. (21)) and becomes independent of f for $R_{BCS} \ll R_{res}$. At $T = 2$ K the BCS term dominates above 3 GHz and here the losses grow linearly with frequency, whereas below 300 MHz

[8]In normal-conducting linacs like SLAC the travelling wave mode may be chosen. Basically the electrons 'ride' on the crests of the rf wave which propagates with the speed of light. In a superconducting linac a travelling wave is not attenuated by wall losses, and in order to preserve the basic advantage of superconductivity - almost no rf power is wasted - one would have to extract the rf wave after some length and feed it back through a superconducting wave guide to the input coupler. The required precision in rf phase would be extremely demanding and would make such a system far more complicated than a standing-wave linac.

the residual resistance dominates and the losses are proportional to $1/f$. To minimize power dissipation in the cavity wall one should therefore select f in the range 300 MHz to 3 GHz. Cavities in the 350 to 500 MHz regime are commonly used in electron-positron storage rings. Their large size is advantageous to suppress wake field effects and losses from higher order modes. However, for a linac of several 10 km length the niobium and cryostat costs would be prohibitive for these bulky cavities, hence a higher frequency has to be chosen. Considering material costs $f = 3\,\mathrm{GHz}$ might appear the optimum but there are compelling arguments for choosing about half this frequency.

- The wake fields generated by the short electron bunches depend on radius as $1/r^2$ for longitudinal and as $1/r^3$ for transverse wakes. Since the iris radius of a cavity is inversely proportional to its eigenfrequency, the wake field losses scale with the second resp. third power of the frequency. Beam emittance growth and beam-induced cryogenic losses are therefore much higher at 3 GHz.
- The f^2 dependence of the BCS resistance makes a 3 GHz cavity thermally unstable at gradients above 30 MV/m, hence choosing this frequency would preclude a possible upgrade of the TESLA collider to 35 MV/m [10].

3.6 Heat conduction in niobium and heat transfer to the liquid helium

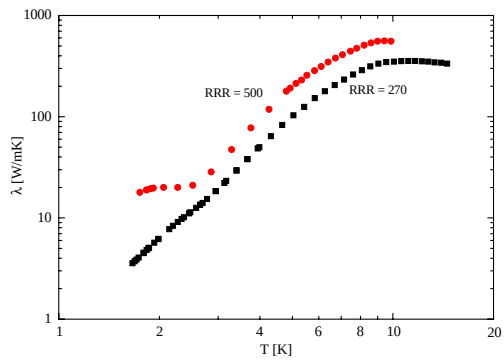

Figure 11: *Measured heat conductivity in niobium samples with RRR = 270 and RRR = 500 as a function of temperature [20].*

The heat produced at the inner cavity surface has to be guided through the cavity wall to the superfluid helium bath. At 2 - 4 K, impurities have a strong impact on the thermal conductivity of metals. Niobium of very high purity is needed (contamination in the ppm range). The heat conductivity drops by about an order of magnitude when lowering the temperature from 4 to 2 K, as shown in Fig. 11. The residual resistivity ratio $RRR = R(300K)/R(10K)$ is a good measure for the purity of the material: large RRR means high electrical and thermal conductivity at low temperature.

The beneficial effect of a high thermal conductivity on the cavity performance is demonstrated in Fig. 12. Here the quality factor Q_0 is plotted as a function of the accelerating field E_{acc} for a nine-cell TESLA cavity before and after a 1400°C heat treatment. The RRR of the niobium increases during this treatment from 380 to 760, and obviously the cavity can be excited to higher fields afterwards. What one can also observe in this figure is a drop of the quality factor towards high fields. The main reason is in this case the onset of electron field emission (see below). These electrons are accelerated in the rf field and impinge on the cavity walls where they deposit energy and may even generate X rays by bremsstrahlung.

Low frequency cavities (350-500 MHz) have a small BCS surface resistance at 4.2 K and are effectively cooled by normal liquid helium. The heat flux should not exceed a few $\mathrm{kW/m^2}$ to obtain nucleate boiling with a close contact between liquid and metal. At higher heat fluxes one enters the film boiling regime where a vapour film covers the surface. Here the cavity may easily warm up beyond T_c at areas of excessive

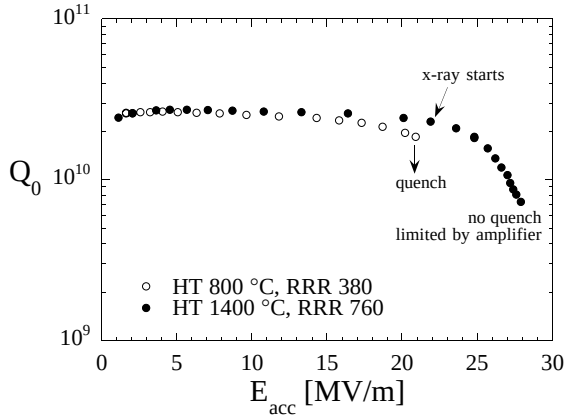

Figure 12: *The excitation curve $Q_0 = Q_0(E_{acc})$ of a nine-cell TESLA cavity before and after the heat treatment at 1400°C.*

heating. The f^2 dependence of the BCS resistance implies that for cavities of higher frequency superfluid helium at 1.8 - 2 K is more appropriate. At the metal-helium interface a temperature jump is observed which is attributed to phonon mismatch. The so-called Kapitza resistance amounts to about $1.5 \cdot 10^{-4}$ $\mathrm{m^2K/W}$ [21] for a clean niobium surface in contact with superfluid helium.

3.7 Maximum accelerating field

Superconductivity breaks down when the microwave magnetic field at the cavity surface exceeds a critical value. The situation is clearcut for a type I superconductor such as lead where the superconducting state prevails up to $B_c = 80$ mT. For the type II conductor niobium it is not so obvious which of the critical fields should be used. The values at 2 K are approximately

- $B_{c1} = 160$ mT
- $B_c = 190$ mT
- $B_{c2} = 300$ mT

A very safe value would be B_{c1} because then no magnetic flux enters the bulk niobium. The corresponding gradient of 38 MV/m in TESLA-type cavities has been definitely exceeded in single-cell cavities, more than 40 MV/m have been repeatedly reached. There is some evidence that the maximum tolerable rf magnetic field is close to the thermodynamic critical field of 190 mT but the issue is not finally settled yet.

The most promising road towards the ultimate gradient is a cavity surface preparation by electrolytic polishing. In figure 13 we show the performance of several electropolished cavities. These results prove that a centre-of-mass energy of 800 GeV can indeed be reached in the TESLA electron-positron collider.

3.8 Thermal instability and field emission

The fundamental advantage of superconducting cavities is their extremely low surface resistance of about 10 nΩ at 2 K, leading to rf losses which are 5 to 6 orders of magnitude lower than in copper cavities. The drawback is that even tiny surface contaminations are potentially harmful as they decrease the quality factor and may even lead to a thermal breakdown (quench) of the superconductor due to local overheating. Temperature mapping at the outer cavity wall usually reveals that the heating is not uniform over the whole surface but that certain spots exhibit larger temperature rises, often beyond the critical temperature of the superconductor. Hence the cavity becomes partially normal-conducting, associated with strongly enhanced power dissipation. Because of the exponential increase of surface resistance with temperature this may result

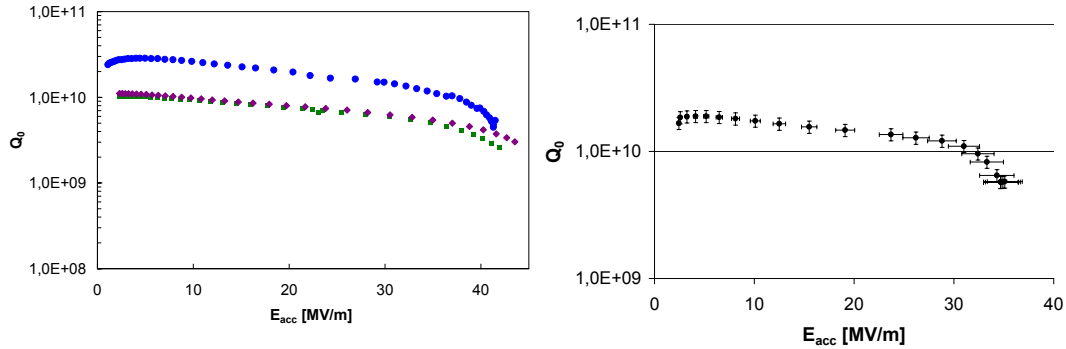

Figure 13: *Excitation curves of electropolished cavities at a helium temperature of 2 K. Left: 1-cell cavities, right: 9-cell cavity.*

in a run-away effect and eventually a quench of the entire cavity. Analytical models and numerical codes are available to describe this effect. The tolerable defect size depends on the purity of the material. As a typical number, the diameter of a normal-conducting spot must be less than 50 μm to avoid a thermal instability at 25 MV/m.

Field emission of electrons from sharp tips has been a notorious limitation of high-gradient sc cavities. The typical indication is that the quality factor drops exponentially above a certain threshold field, and X rays are observed. The field emission current density is given by the Fowler-Nordheim equation [23], adapted for rf fields:

$$j_{FE} \propto \frac{E_{loc}^{2.5}}{\Phi} \exp(-C\Phi^{3/2}/E_{loc}) \; . \tag{43}$$

Here Φ is the work function of the metal, C a constant and E_{loc} the local electric field. At sharp tips on the surface the local field may be several 100 times larger than the accelerating field. Perfect cleaning by rinsing with high-pressure ultrapure water is the most effective remedy against field emission. Using the clean room techniques developed in semiconductor industry it has been possible to raise the threshold for field emission in multicell cavities from about 10 MV/m to more than 20 MV/m in the past few years. Thermal instabilities and field emission are discussed at much greater detail in [10].

References

[1] P. Schmüser, *Superconductivity in High Energy Particle Accelerators*, Prog. Part. Nucl. Phys. 49 (2002) issue 1. Available from the internet: http://wwww.desy.de/∼pschmues , file supercon-acc.pdf

[2] Review of Particle Properties, Europ. Phys. Journ. **C15** (2000)

[3] C. Adolphsen *et al.*, SLAC Report 474 (1996)

[4] JLC Design Study, KEK Report 97-1 (1997)

[5] G. Guignard *et al.*, CERN Report 2000-008 (2000)

[6] B.H. Wiik, Part. Acc. 62 (1998) 563

[7] TESLA, Technical Design Report, The Accelerator, Eds. R. Brinkmann, K. Flöttmann, J. Rossbach, P. Schmüser, N. Walker, H. Weise, DESY report 2001-23 (2001)

[8] G.A. Krafft, *Status of the Continuous Electron Beam Accelerator Facility*, Proc 1994 Linear Accel. Conf., 9 (1994)

[9] International Linear Collider Technical Review Committee Report II (2002), ed. G.A. Loew, to be published

[10] H. Padamsee, J. Knobloch and T. Hays, *RF Superconductivity for Accelerators*, John Wiley, New York 1998.

[11] H. Piel in: Proc. of the 1988 CERN Accelerator School *Superconductivity in Particle Accelerators*, CERN report 89-04 (1989)

[12] D.C. Larbalestier and P.J. Lee, Proc. PAC99, New York (1999) 177

[13] W. Buckel, *Supraleitung*, VCH Verlagsgesellschaft, Weinheim 1990

[14] D.R. Tilley and J. Tilley, *Superfluidity and Superconductivity*, Institute of Physics Publishing Ltd, Bristol 1990

[15] E.W. Collings *et al.*, Adv. Cryog. Eng. **36** (1990) 169

[16] G. Müller, Proc. 3rd Workshop on RF Superconductivity, ed. K.W. Shepard, Argonne, USA (1988), p. 331

[17] B. Bonin, CERN Accelerator School *Superconductivity in Particle Accelerators*, CERN 96-03, ed. S. Turner, Hamburg (1995)

[18] J. Halbritter, Z. Physik **238** (1970) 466

[19] C. Benvenuti *et al.*, Proc. PAC91, San Francisco (1991), p. 1023.

[20] T. Schilcher, TESLA-Report, TESLA 95-12, DESY (1995)

[21] A. Boucheffa *et al.*, Proc. 7th Workshop on RF Superconductivity, ed. B. Bonin, Gif-sur-Yvette, France (1995), p. 659

[22] B. Aune *et al.*, Phys. Rev. Spec. Top. Acc. Beams PRSTAB 3 (2000) 092001

[23] R.H. Fowler and L. Nordheim, Proc. of the Roy. Soc. A 119, 173 and Math. Phys. Sci. 119 (1928) 173.